



ELSEVIER

Available online at [www.sciencedirect.com](http://www.sciencedirect.com)

SCIENCE @ DIRECT®

Ore Geology Reviews 22 (2003) 177–199

ORE GEOLOGY  
REVIEWS

[www.elsevier.com/locate/oregeorev](http://www.elsevier.com/locate/oregeorev)

# Post-collisional crustal extension setting and VHMS mineralization in the Jinshajiang orogenic belt, southwestern China

Hou Zengqian<sup>a</sup>, Wang Liquan<sup>b</sup>, Khin Zaw<sup>c,\*</sup>, Mo Xuanxue<sup>d</sup>, Wang Mingjie<sup>b</sup>,  
Li Dingmou<sup>b</sup>, Pan Guitang<sup>b</sup>

<sup>a</sup>*Institute of Mineral Resources, Chinese Academy of Geological Sciences, Beijing 100037, PR China*

<sup>b</sup>*Chengdu Institute of Geology and Mineral Resources, Chengdu 56000, PR China*

<sup>c</sup>*Centre for Ore Deposit Research, University of Tasmania, GPO Box 252-79, Hobart 7001, Australia*

<sup>d</sup>*China University of Geosciences, Beijing 100082, PR China*

Received 11 March 2002; accepted 25 October 2002

## Abstract

The Jinshajiang orogenic belt (JOB) of southwestern China, located along the eastern margin of the Himalayan–Tibetan orogen, includes a collage of continental blocks joined by Paleozoic ophiolitic sutures and Permian volcanic arcs. Three major tectonic stages are recognized based on the volcanic–sedimentary sequence and geochemistry of volcanic rocks in the belt. Westward subduction of the Paleozoic Jinshajiang oceanic plate at the end of Permian resulted in the formation of the Chubarong–Dongzhulin intra-oceanic arc and Jamda–Weixi volcanic arc on the eastern margin of the Changdu continental block. Collision between the volcanic arcs and the Yangtze continent block during Early–Middle Triassic caused the closing of the Jinshajiang oceanic basin and the eruption of high-Si and -Al potassic rhyolitic rocks along the Permian volcanic arc. Slab breakoff or mountain-root delamination under this orogenic belt led to post-collisional crustal extension at the end of the Triassic, forming a series of rift basins on this continental margin arc. Significant potential for VHMS deposits occurs in the submarine volcanic districts of the JOB. Mesozoic VHMS deposits occur in the post-collisional extension environment and cluster in the Late Triassic rift basins.

© 2002 Elsevier Science B.V. All rights reserved.

*Keywords:* VHMS deposits and mineralization; Post-collisional crustal extension; The Jinshajiang orogenic belt; Southwestern China

## 1. Introduction

Volcanic-hosted massive sulfide (VHMS) deposits occur mainly in three tectonic settings: (1) intra-arc rifts or back-arc basins containing marine bimodal volcanic complexes and Kuroko-type deposits (Frank-

lin et al., 1981; Cathles et al., 1983; Halbach et al., 1989; Urabe and Marumo, 1992; Fouquet et al., 1993), (2) extensional intra-continental or continent-marginal rift depressions dominated by felsic magmatism that have a spectrum of VHMS deposits with variable Cu/Pb + Zn ratios, and (3) spreading oceanic-ridges containing Cu or Cu–Zn deposits (Rona, 1984; Rona and Scott, 1993). Recent research on metallogeny of these deposits indicated that metallogenic processes of VHMS deposits also occur extensively in

\* Corresponding author. Fax: +61-3-62232547.

E-mail address: [Khin.Zaw@utas.edu.au](mailto:Khin.Zaw@utas.edu.au) (K. Zaw).

a post-collisional crustal extension setting in addition to volcanic arcs or back-arc basins (Crawford and Berry, 1992; Crawford et al., 1992, 2000). The Jinshajiang orogenic belt (JOB), in the Sanjiang Tethysan domain in southwestern China, is a typical example. The VHMS deposits of the JOB occur in post-collisional extensional rift basins formed at the end of the Triassic. This paper presents a new geodynamic setting for VHMS deposits, based on the latest geological and litho-geochemical data obtained in the JOB.

## 2. Regional geological setting of the JOB

The JOB is located along the eastern margin of the Himalayan–Tibetan Orogen (Sengor and Natalin, 1996; Yin and Harrison, 2000) and includes the Changdu continental block, Paleozoic ophiolitic sutures (Jinshajiang) and a volcanic–plutonic arc (Jamda–Weixi arc) (see Fig. 1b; Mo et al., 1993; Liu et al., 1993). The belt is 60-km wide and more than 1000 km long, extending from Eastern Tibet through Western Sichuan to Western Yunnan (Fig. 1). The belt is also divided into four secondary structure zones. From east to west, these comprise a foreland fold belt and thrust zone, an ophiolite melange zone, a superimposed rifting basin zone and a continent–marginal volcanic arc zone (Fig. 1; Wang et al., 1999a).

The foreland fold belt and thrust zone is located on the western margin of the Zongza continental block and comprises Early Paleozoic carbonates, turbidites, basic lavas and volcanoclastic units. The succession forms eastward-thrusting structural slabs or folded zones with broadly EW-trending axes.

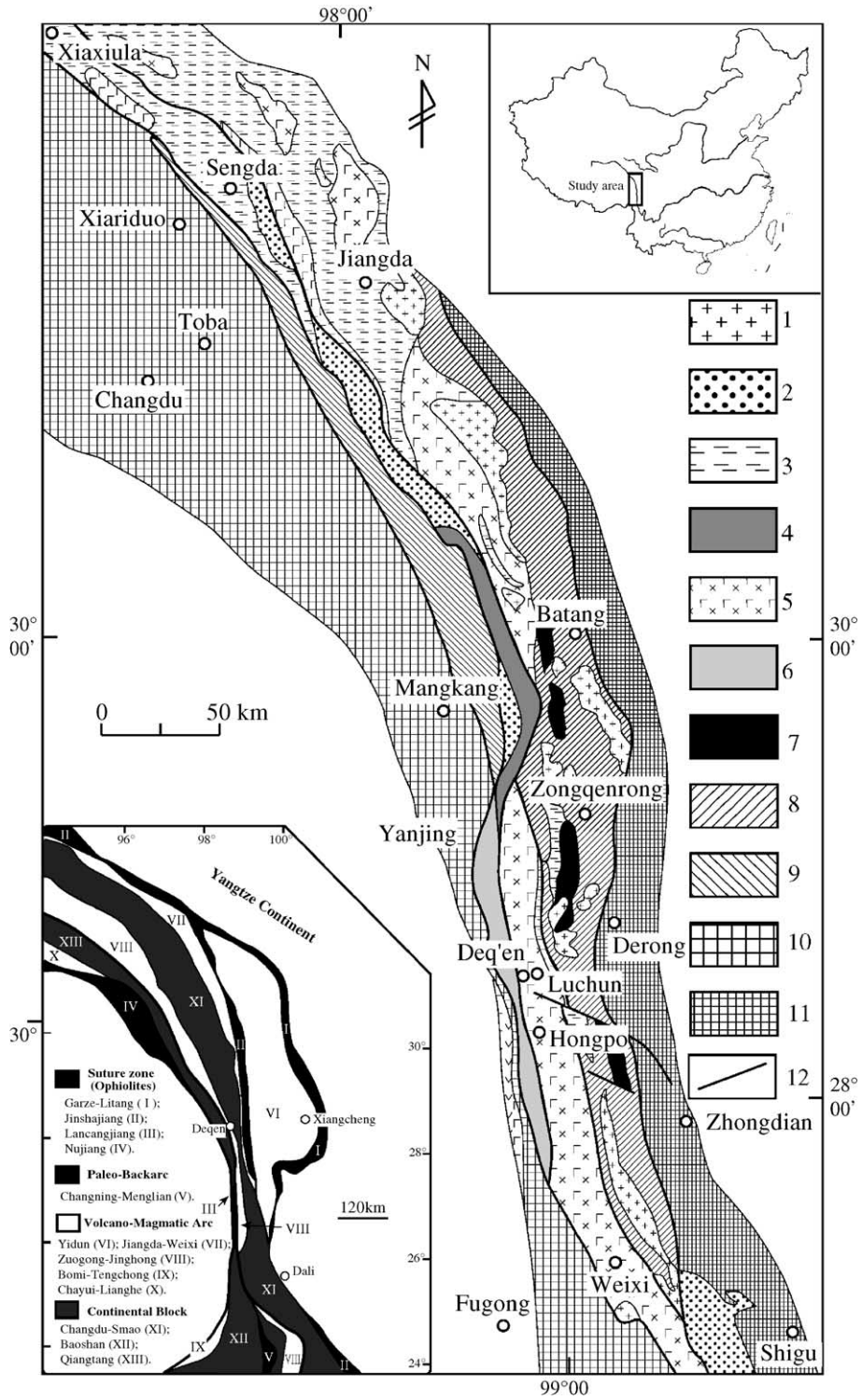
The ophiolitic melange zone is 20–40-km wide and over 1000-km long, and extends from Shiqu, Qinghai Province in the north to Jinping, Yunnan Province, in the south (Fig. 1b). The ophiolite and ophiolitic melange is discontinuously distributed along this zone and is intercalated with minor Permian

limestone fragments from the Zongza continental block. The melange zone is unconformably overlain by Late Triassic red beds. The eastern part of the melange zone contains a typical ophiolitic suite, comprising lower mafic–ultramafic rocks, mid-ocean ridge basalt (MORB) and ocean–island basalt (OIB), diabase dikes, plagiogranites and radiolarian siliceous rocks (Mo et al., 1993; Hou et al., 1996a,b). The lower and upper basic lavas yielded zircon U–Pb ages of 361.6 and 269.1 Ma, respectively (Zhan et al., 1998). The plagiogranites also yield similar U–Pb ages from  $340 \pm 3$  to  $294 \pm 3$  Ma (Wang et al., 1999b). The western part of the melange zone consists mainly of ophiolite, relics of oceanic crust and intra-oceanic arc volcanics. Rb–Sr isochron ages of these melanges range from 268.7 to 257.1 Ma (Wang et al., 1999a). Clastic rocks and siliceous slate are also present in the zone.

The continental margin arc zone forms a major component of the JOB, and is dominated by Permian arc volcanic–sedimentary sequences, at the eastern margin of the Changdu continental block (Fig. 1). The continental margin arc, over 100-km long, extends from Jamda in the north to Weixi in the south (Fig. 1). Tholeiitic, calc-alkaline and shoshonitic volcanic and intrusive rocks developed successively along this volcanic–magmatic arc. Folded Proterozoic–Early Paleozoic crystalline rock form basement to the continental block, which is in turn overlain by late Paleozoic–Mesozoic rocks. The Proterozoic crystalline basement comprises of a suite of lower amphibolite and upper greenschist facies metamorphic rocks. Similar rocks are present in the basement of the Yangtze continent. Early Paleozoic folded basement is characterized by flyschoid sedimentary formations, and the sedimentary facies are similar to those of the Yangtze continent. The late Paleozoic cover consists primarily of extensive platform transitional facies carbonate and clastic rocks.

The extensional rifting zone is superposed on the Permian Jamda–Weixi arc (Fig. 1). The southern segment of this zone is filled by Late Triassic bimodal

Fig. 1. Sketch showing tectonic framework and the distribution of volcanic rocks in the Jinshajiang orogenic belts (JOB). 1. Indosinian–Yanshanian granites; 2. Tertiary red beds; 3. Upper Triassic clastic sedimentary rocks; 4. Volcanic rocks of the arc–continent collision stage ( $T_{1-2}$ ); 5. Volcanic rocks of the Late Triassic extensional rifting–subsidence stage; 6. Permian continental margin arc volcanic rocks; 7. Permian intra-oceanic arc volcanic rocks; 8. Jinshajiang structural melange belt; 9. Qingnitong–Haitong thrust–nappe belt; 10. Changdu continental block; 11. Zongza continental block; 12. Fault.



volcanic rocks and turbidite and microclastic sequences, suggesting a bathyal environment (Wang et al., 1999a). The northern segment of the zone has two rift basin branches. The eastern branch occurs in the Jiamda–Dingqinnong region (Fig. 1), where calc-alkaline intermediate to felsic volcanic rocks as well as carbonate and siltstone are present. The sedimentary facies suggest a shallow-water environment. The western branch near the Chasuo–Shengda region (Fig. 1) comprises Late Triassic submarine pillow basalts and marine-bathyal flysch sediments consisting of slate interbedded with limestone.

### 3. VHMS deposits and mineralization

The VHMS deposits in the JOB occur mainly in two important marine volcanic districts, i.e., Batang–Deqen and Jamda–Deqen–Weixi districts. There are three major mineralized horizons, which comprise an important massive base-metal sulfide ore belt (Figs. 2–4, Table 1).

#### 3.1. Batang–Deqen marine volcanic district

In the Permian arc volcanic district, two tectono-strata units have been recognized, i.e., Paleozoic ophiolitic melange and Devonian–Permian calc-alkaline volcanic–sedimentary sequence (Fig. 3; Zhan et al., 1998). The VHMS deposits occur in lower metamorphosed calc-alkaline volcanic district, and are hosted by Early Permian andesitic rocks that are overlain by siliceous phyllitic slate, sandstone and carbonate. These deposits record the earliest epoch of sulfide mineralization in the orogenic belt.

*Yagra deposit:* Yagra copper deposit is the largest known VHMS deposit with more than 0.7 Mt Cu reserves in the volcanic district. In the Yagra district, Paleozoic volcanic–sedimentary sequence is composed of the Devonian marble and sandstone on the bottom, the Carboniferous tholeiitic basalts in the middle part and Permian calc-alkaline basaltic andesite and andesite and associated chert, siliceous slate and carbonate in the upper part. The sequence was intruded by granitic diorite and monzogranite intrusions with Rb–Sr isochron ages ranging from 208.3 to 227.1 Ma (Zhan et al., 1998). Accompanying with sulfide mineralization, calc-alkaline volcanic rocks

was affected by hydrothermal alteration, such as silicification, chloritization, sericitization and carbonatization (Wei et al., 1999).

Yagra deposit is mainly composed of the upper massive sulfide zone and the underlying stringer-stockwork zone (Fig. 5). The massive sulfide zone is made up of a series of tabular sheets or ore lens dipping about 25°W; these ore lenses have various thicknesses from 2.2 to 64 m and extend over a 1600-m strike length (Fig. 5). They are hosted in andesitic rocks and associated siliceous slate and are overlain conformably by carbonate rocks, pyrite black shale and chert (Fig. 5), showing obviously strata-bound characteristic. The crosscutting stringer-stockwork zone extends virtually almost the entire length below thin and extensive sheet of layered massive sulfide zone, and is characteristic stratabound polymetallic zone rather than pyrite–chalcopyrite pipe (Fig. 5). The ore mineral assemblages are dominantly chalcopyrite, pyrrhotite, pyrite, sphalerite, galena and with minor magnetite, chalcocite, tetrahedrite and bornite.

It is worthy to note that late emplacement of granite intrusions not only led to host volcanic–sedimentary sequence to skarnification, but also resulted in copper mineralization to form chalcopyrite–quartz vein swarms, overprinted on massive sulfide orebodies in the district (Fig. 5).

#### 3.2. Jamda–Deqen–Weixi volcanic districts

VHMS deposits in the Deqen–Weixi district are associated with Late Triassic submarine felsic volcanic complexes in a rift basin. In bimodal volcanic district, a number of sulfide deposits including mineralized occurrences and prospects have been discovered (Fig. 3, Table 1). The host rocks are rhyolitic volcanic piles, which yielded a Rb–Sr isochron age of 238.9 Ma (Wang et al., 1999a). These deposits are mostly stratiform or stratabound and are closely associated with lamellar chert and banded dolomite.

*Luchun deposit:* The Luchun deposit, the largest (>0.5 Mt Cu) known VHMS deposit in the volcanic district, lies in the Late Triassic Jijiang basin that was filled by a volcanic–sedimentary sequence of the Renzhixueshan Formation, characterized by bimodal volcanic suite (Fig. 6). The sulfide orebodies were hosted in rhyolitic volcanic package, which is composed of a series of complex volcanic centers with

System	Series	Columnar Section	Ore-bearing Horizon	Volcanic Rock Association	Sedimentary Facies	Tectonic Setting	Isotopic Age
Triassic	Upper member of Upper Triassic		Zhaokalong -style Fe-Ag-Pb-Zn deposits	Potassic calc-alkaline, andesite-dacite-rhyolite	Bioclastic limestone Shallow-sea volcanic depression Shallow-sea limestone sediments molasse clastic facies	Shrinking stage of basins	Rb-Sr 235-238 Ma
	Lower member of Upper Triassic		Luchun-style Cu-Zn-Pb deposits	rhyolite Bimodal (basalt-rhyolite) suite Tholeiite and basaltic pyroclastic rocks	Sub-deep-sea sandy mudstone Sub-deep-sea volcanic sedimentary basin Bottom tuffaceous turbidite	Rifting stage of basins	
	Middle Lower Triassic			High-K and high-Si rhyolitic volcanics		Arc-continent collision, Foreland basin	
Permian	Upper member of Upper Permian			Basaltic andesite-andesite-dacite-rhyolite in the continental-margin		Continental-margin arc	K-Ar 257.1-268.7 Ma
	Lower member of Upper Permian		Yagra-style Cu-Zn deposits	Basalt-basaltic andesite in the intra-oceanic arc	Sub-deep-sea siliceous sandy-muddy flysch	Intra-oceanic arc	
Carboniferous				MORB	Deep-sea siliceous rock facies	Spreading oceanic basin	U-Pb 296.1 Ma 361.6 Ma

Fig. 2. Tectono-stratigraphic units and major VHMS-bearing horizons in the Jinshajiang orogenic belt (JOB).

related epiclastic facies, which were suffered from silicification, sericitization and chloritization. The favorable horizon or ore equivalent horizon (Large, 1992) within the host volcanic pile is an exhalative sequence consisting of layered cherts with subordinate dolomitic limestone lens and pyrite black shale.

Due to strong erosion and deformation, the sulfide zones outcrop at three segments in the Luchun districts (Fig. 6). The main sulfide zones are made up of

a series of tabular sheets or lens dipping 25° to 40°E. The individual ore lenses strictly occur in rhyolitic tuff and tuffaceous slate strata of the bimodal suite, and are obviously stratabound (Fig. 6). Sulfide orebodies are predominated by massive ores, showing obvious variation in texture and structure from laminated, banded ores to massive and breccia ores. The stock-work-stringer ores are subordinate, and occur underneath massive sulfide zone or margins of the massive

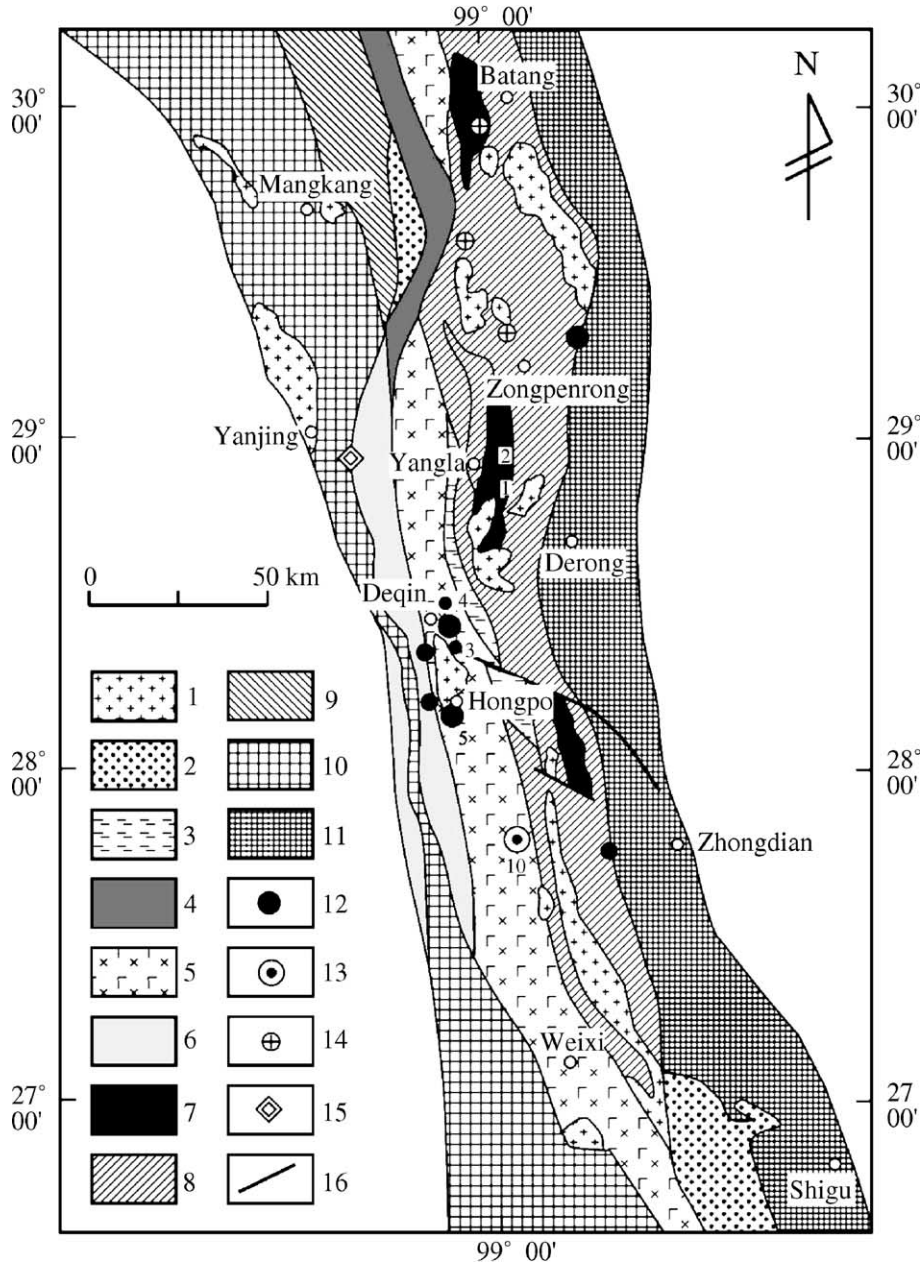


Fig. 3. Tectono-magmatic framework of the southern segment of the JOB and the distribution of deposits (after Li et al., 2000). 1. Indosinian–Yanshanian granites; 2. Tertiary red beds; 3. Upper Triassic clastic sedimentary rocks; 4. Volcanic rocks of the arc–continent collision stage (T1–2); 5. Volcanic rocks of the Late Triassic extensional rifting stage; 6. Permian continental margin arc volcanic rocks; 7. Permian intra-oceanic arc volcanic rocks; 8. Jinshajiang structural melange belt; 9. Qingnitong–Haitong thrust–nappe belt; 10. Changdu continental block; 11. Zongza continental block; 12. Cu (-Zn) deposit and occurrence; 13. Ag-polymetallic siderite deposit; 14. Au deposit and occurrence; 15. Gypsum deposit. The number of the Cu (-Zn) deposits in the figure is same as that in Table 1.

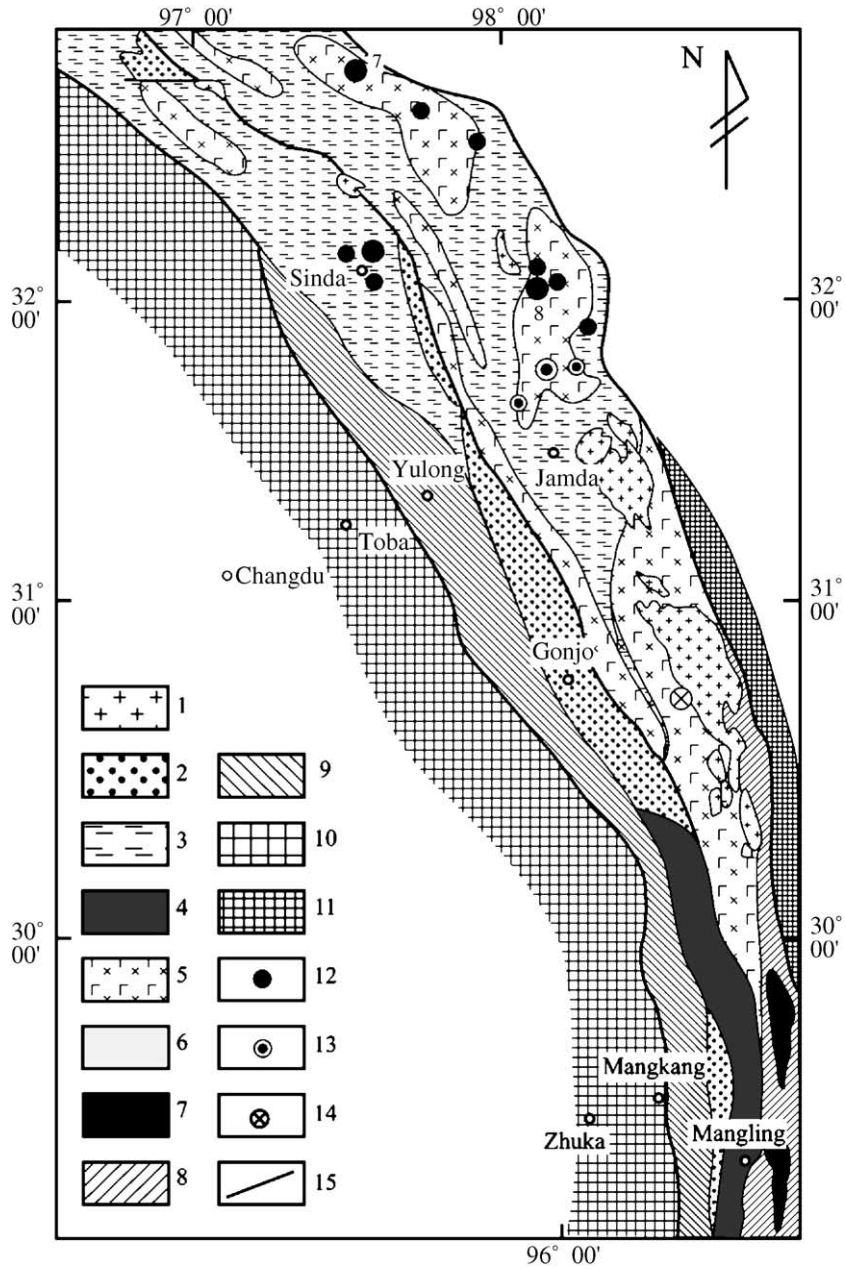


Fig. 4. Tectono-magmatic-metallogenic map of the northern segment of the Jinshajiang orogenic belt (after Wang et al., 2000). 1. Indosinian–Yanshanian granites; 2. Tertiary red beds; 3. Upper Triassic clastic sedimentary rocks; 4. Volcanic rocks of the arc–continent collision stage (T1–2); 5. Volcanic rocks of the Late Triassic extensional rifting stage; 6. Permian continental margin arc volcanic rocks; 7. Permian intra-oceanic arc volcanic rocks; 8. Jinshajiang structural melange belt; 9. Qingnitong–Haitong thrust–nappe belt; 10. Changdu continental block; 11. Zongza continental block; 12. Ag-polymetallic deposits; 13. Skarn- and porphyry-type Fe deposits; 14. Pb–Zn deposit; 15. Fault. The number of the Ag-polymetallic deposits (7, 8) in the figure is same as that in Table 1.

Table 1

Representative VHMS deposits in the Jinshajiang orogenic belt and their mineralization characteristics

Ser. no.	Ore deposit	Tectonic setting interpretation	Geological age of host rocks	Host rocks	Exhalative rocks	Morphology of orebody
1	Yagra, Deqen	Intra-ocean arc	End of Early Permian, Early Late Permian	Hornblende andesitic volcanic rocks interbedded with siliceous sericitic slate, bedded skarn	Pyrite black shale, chert	Stratiform, lenticular, stringer-stockwork
2	Geyading, Deqen	Intra-ocean arc	End of Early Permian–Early Late Permian	Basaltic andesite–hornblende andesitic pyroclastic rocks	Unknown	Lenticular, stockwork
3	Luchun, Deqen	Extensional rifting basin	Late Triassic	Rhyolitic breccia tuff in the bimodal suite	Chert, pyrite black shale, tuffaceous slate thin-bedded dolomitic limestone	Bedded, stratiform, lenticular
4	Buyanlacha, Deqen	Extensional rifting basin	Late Triassic	Rhyolitic volcanic rocks in the bimodal suite	Chert, pyrite black shale, tuffaceous slate thin-bedded dolomitic limestone	Bedded, banded
5	Hongpo, Deqen	Extensional rifting basin	Late Triassic	Massive rhyolite and underlying siliceous Sericitic slate	?	Stratabound, massive, disseminated
6	Xioruo, Deqen	Extensional rifting basin	Late Triassic	Bimodal basalt–rhyolite association, rhyolitic pyroclastic rocks	Unknown	Disseminated, stockwork
7	Zhaokalong, Qinghai	Extensional rifting basin	Late Triassic	Andesite, andesitic tuff breccia, tuff, overlying limestone and sandy slate	Bedded siderite rock, medium–thin-bedded dolomite	Banded, stratiform, lenticular and lumpy within banded siderite
8	Dingqinnong, East Tibet	Extensional rifting basin	Late Triassic	Dacitic pyroclastic rocks, secondary quartzite and overlying medium–thick-bedded marble	Bedded-lenticular siliceous rocks, medium–thin-bedded dolomite	Stratoid, banded, disseminated, stockwork
9	Jiangpo, Deqen	Extensional rifting basin	Late Triassic	Dacitic pyroclastic rocks and overlying sandy slate and limestone	Bedded siderite rock, Hematite chert	Bedded, stratabound, lenticular
10	Chugezha, Deqen	Extensional rifting basin	Late Triassic	Dolomitic limestone in the upper felsic volcanic rocks,	Bedded siderite rock, Hematite cherts	Bedded, stratabound, lenticular

Py: pyrite; Sp: sphalerite; Gn: galena; Mt: magnetite; Cp: chalcopyrite; Sid: siderite; He: hematite; It: ilmenite; Spe: specularite.

orebody. The ore minerals are dominantly pyrite, sphalerite, galena and chalcopyrite, with minor magnetite, arsenopyrite, pyrrhotite, bournonite, boulangerite and ilmenite.

In the Jamda volcanic district, VHMS deposits are mainly hosted in the Late Triassic calc-alkaline intermediate-felsic volcanics and in the contact zones between overlying thickly bedded micrite and medium to thinly bedded greyish green sandstone. Disseminated, stringer-stockwork and lenticular orebodies occur within the stratified siderite-rich beds,

and are closely associated with barite-rich cherts. VHMS deposits from the volcanic district include the Zhaokalong and Dingqinnong Fe–Ag-polymetallic deposits and the Chugezha Fe–Ag deposit (Table 1).

*Zhaokalong deposit:* The Fe–Ag polymetallic deposit, a typical, large-size deposit with more than 2000 T Ag, occurs in the Jamda felsic volcanic district. The host volcanic–sedimentary sequence is composed of basal thick gray limestone ( $T_3^1$ ), lower green andesite and sandy slate and dolomite ( $T_3^2$ ), and

Metal assemblage	Metal zonation	Ore mineral	Ore structure	Alteration	Major reference
Cu–(Zn–Pb) or Cu–Zn	None obvious	Py, Po, Cp, chalcocite, tetrahedrite, bornite, galena, sphalerite	Massive, banded, breccia, laminar, stringer-stockwork,	Silicification, sericitization, chloritization, montmorillonization,	Zhan et al., 1998; Chen et al., 1998; Wei et al., 1999
Cu–(Zn)	Unknown	Py, Cp, Po, marcasite	Massive, stockwork	Silicification, sericitization, chloritization	Li et al., 2000
Cu–Zn	None obvious	Py, Cp, Mt, It, Cc, Bn, Gn, Sp	Massive, laminar, banded, stringer-stockwork, graded bedding	Silicification, sericitization, chloritization	Wang et al., 1999a; Li et al., 2000
Cu–Zn	None obvious	Py, Cp, Ga, Sp	Massive, banded	Silicification, sericitization, chloritization	Li et al., 2000
Cu–Au	Cu–Au in the lower, Cu–Pb–Zn in the upper	Py, Cp, Gn, Sp, Mt	Massive, disseminated	Silicification, sericitization	Li et al., 2000
Cu–Au	None obvious (no massive ore)	Py, Cp, Mt, Sp, Gn	Disseminated, stockwork	Silicification, sericitization, chloritization	Li et al., 2000
Fe–Ag–Pb–Zn	None obvious	Sid, Py, Sp, Gn, He	Laminar, banded, graded bedding, disseminated	silicification, chloritization, epidotization, skarnification	Liu et al., 1993; Ye et al., 1992
Cu–Ag–Pb–Zn	None obvious	Py, Cp, Mt, Ga, Sp, He, Spe	Bedded, banded, disseminated, stockwork	Skarnification, silicification, baritization	Wang et al., 2000
Fe–Ag	None obvious	Sid, He, It, Gn	Bedded, banded, veined	Carbonate alteration, strong silicification,	Li et al., 2000
Fe–Ag	None obvious	Sid, He, It, Gn	Bedded, banded, veined	Carbonate alteration, strong silicification,	Liu et al., 1993

upper sandy-slate and thick layered limestone ( $T_3^3$ ) (Fig. 7). The sulfide orebodies are hosted by 20–50-m-thick siderite beds, which are interpreted to be exhalative sedimentary rocks formed on the top of green andesitic rocks. The stratabound sulfide orebodies are made up of a series of ore lens, 150–300-m long (Fig. 7), and show typical sedimentary structures, e.g., bedded, laminated and graded bedding, etc. The main mineral assemblage is siderite, hematite, ilmenite, galena, pyrite and minor chalcopyrite, sphalerite and native silver.

#### 4. Volcanic–sedimentary sequences and volcanic facies association

The spatial and temporal distribution, rock association and lithofacies characteristics of volcanic rocks from the three major volcanic–sedimentary sequences recognized in the JOB are: (1) Permian arc volcanic–sedimentary sequence, (2) Early–Middle Triassic syn-collisional volcanic–sedimentary sequence and (3) Late Triassic post-collisional volcanic–sedimentary sequence. These three sequences

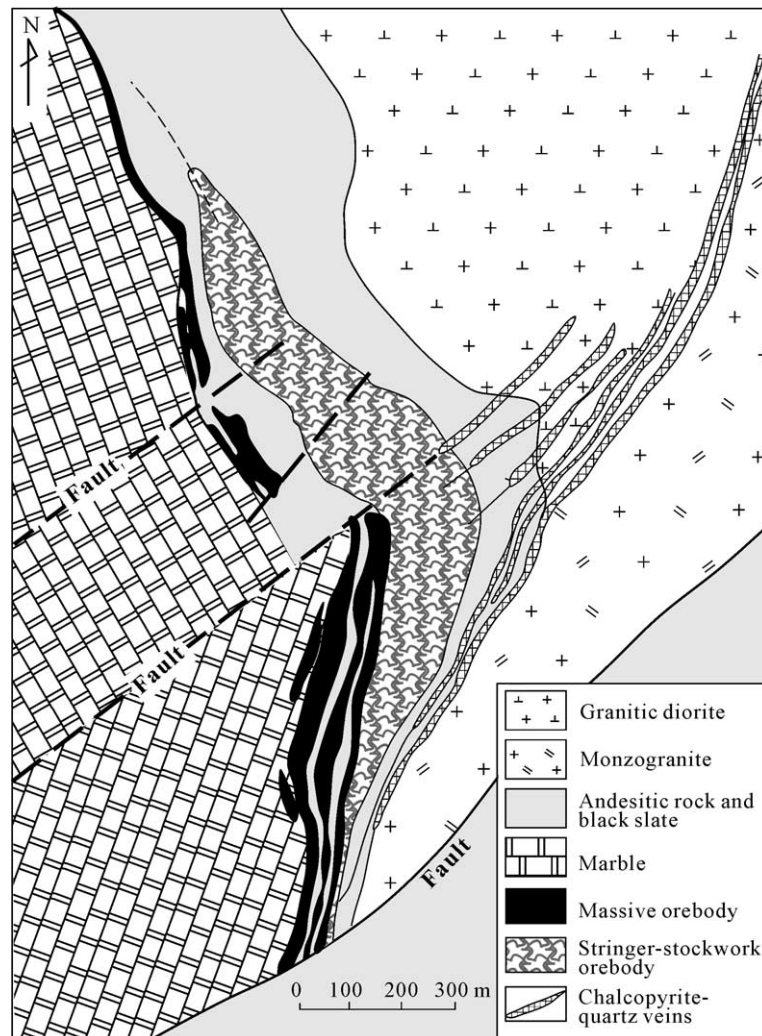


Fig. 5. Simplified geological map of the Yagra copper deposit, Deqin, S.W. China (modified from Li et al., 2000).

are interpreted to represent different tectonic settings, i.e. arc orogeny, arc–continent collision and post-collisional lithospheric extension, and are described below.

#### 4.1. Permian arc volcanic–sedimentary sequence

This Permian arc volcanic–sedimentary sequence occurs at the eastern margin of the Changdu continental block and constitutes two arc volcanic belts: the Chubarong–Dongzhulin intra-oceanic arc vol-

canic belt and the Jamda–Deqen continental margin arc volcanic belt.

In the Chubarong–Dongzhulin belt, the volcanic sequence is up to 600-m thick and conformably overlies on the Carboniferous oceanic succession with isotope ages of 316.6–269.1 Ma (Wang et al., 1999b). It is composed of at least two volcanic–sedimentary units. The lower unit comprises sericitized black shale, and cherts interbedded with medium-to thickly bedded limestone. The upper unit comprises basaltic andesite and andesite, overlain by a succession of

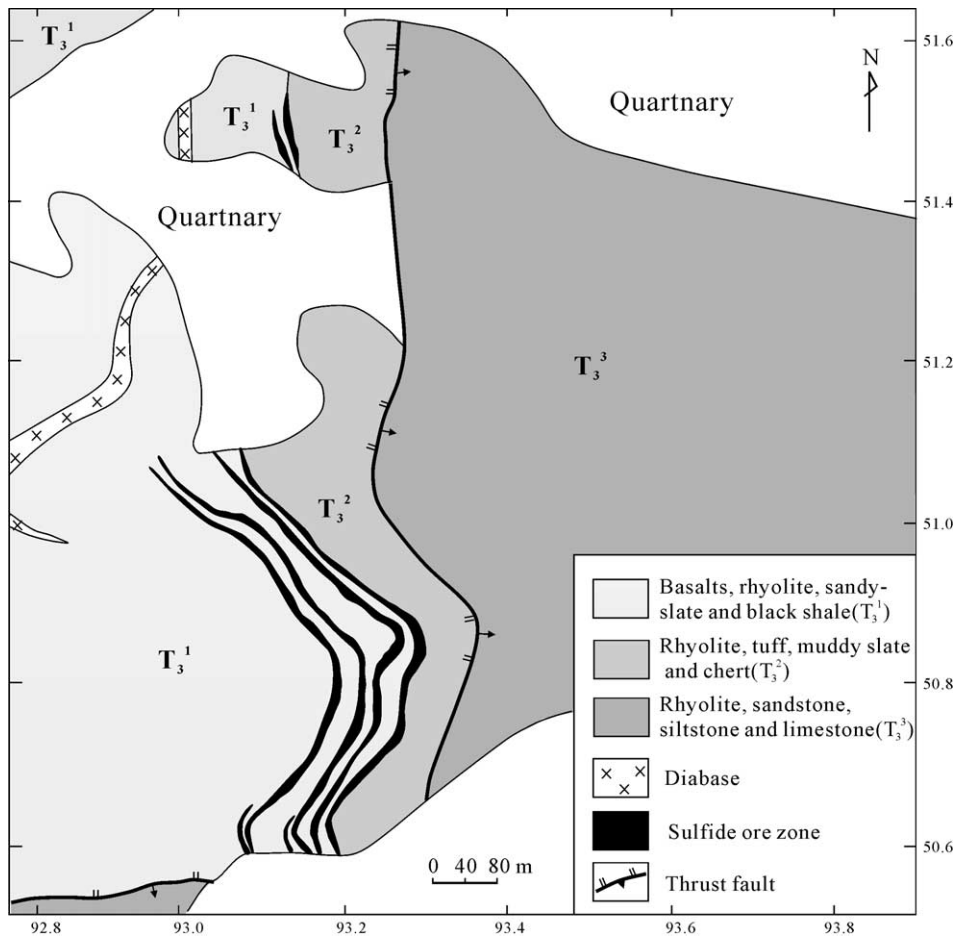


Fig. 6. Simplified geological map of the Luchun copper deposit, Deqin, S.W. China (modified from Li et al., 2000).

thinly bedded sandy slate and/or cherts, and hosts the Yagra-type VHMS deposits. Calc-alkaline andesitic lavas characterize the upper unit.

In the Jamda–Deqen belt, the lower Permian sequence is 2000–2280-m thick and the volcanic succession, comprising pyroclastic rocks and minor lava, is 800–1700-m thick. This sequence has two volcanic–sedimentary units. The lower unit comprises basalt, andesite, dacite and rhyolite with sandy slate, whereas the upper unit is basalt, andesite, and dacite and dacitic pyroclastic rocks with minor shale and carbonate. The upper Permian sequence is up to 500-m thick, consisting mainly of andesitic, dacitic and dacitic–rhyolite lavas and pyroclastic rocks interbedded with thinly bedded silty sandstone, and overlain unconformably by the upper Permian Hongpo Formation.

#### 4.2. Early–Middle Triassic volcanic–sedimentary sequence

This sequence occurs in a small region, from Jamda–Qizhong in the north to Deqen in the south, and uncomfortably overlies on the Permian arc volcanic–sedimentary sequence. In the Jamda–Qizhong area, the sequence unconformably overlies arc granite batholith with a U–Pb age of 246 Ma and a Rb–Sr isochron age of 229 Ma (Liu et al., 1993). It also comprises a lower Triassic volcanic–sedimentary sequence and Middle Triassic deep-water volcanic–sedimentary sequence. The lower Triassic sequence comprises basal coarse-grained arkose and pebble conglomerate, minor shale and carbonate, and felsic volcanic rocks. The volcanic rocks are up to 3000-m

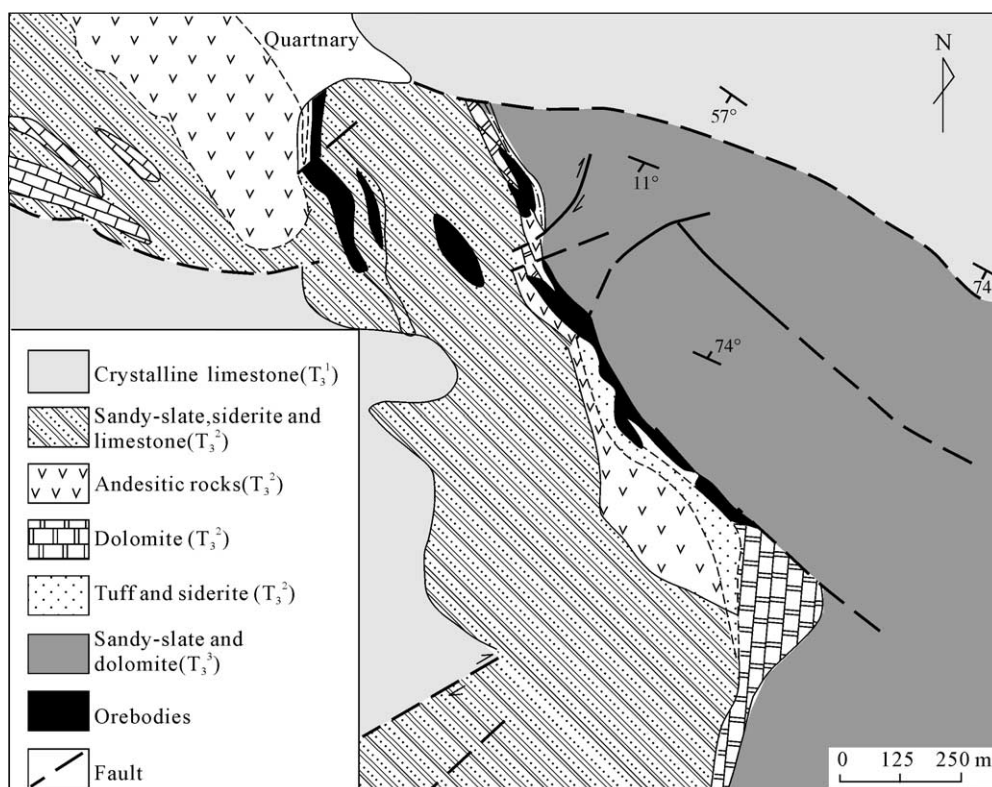


Fig. 7. Simplified geological map of the Zhaokalong Fe–Ag polymetallic deposit, Qinghai province (modified from Wang et al., 2000).

thick and consist of calc-alkaline rhyolite and dacite. The Middle Triassic sequence comprises felsic volcanics up to 2857-m thick and deep-water turbidite facies shale and chert. In the Deqen–Luchun area, the sequence comprises dacitic to rhyolitic volcanics with minor low-grade metamorphic sandy slate. Highly explosive eruptions and shallow intrusions of felsic magmas characterize the Early–Middle Triassic volcanism in the area.

#### 4.3. Late Triassic volcanic–sedimentary sequence

This sequence is associated only with Late Triassic volcano-rift basins. Within the Reshuitang and Jijiading basins in the southern segment of the volcano-rift zone, this sequence is intruded by the underlying granites, and is overlain unconformably by upper Triassic molasses formation. The total thickness of the sequence is between 3200 and 4700 m, and it includes lavas and subordinate pyroclastic rocks. At

least 10 volcanic–sedimentary units have been recognized in this sequence. The lower units are dominated by thickly bedded basaltic lavas, and are interbedded with thinly bedded shale and chert. The middle units comprise basalts in the lower part, calcareous siltstone and limestone in the middle, and 500–1000-m-thick rhyolites in the upper part. The upper units comprise siliceous shale and turbidite in the lower part and rhyolite near the top. The uppermost parts of the basin were filled by a littoral–neritic molasses formation with minor intermediate-felsic volcanic and pyroclastic rocks.

In the northern segment of the volcanic rift zone, the volcanic–sedimentary sequence occurs in the Xialaxiu–Sinda and Zhaokalong–Dingqinlong basins (Fig. 4). The Xialaxiu–Sinda basin unconformably overlies upper Paleozoic strata, and is comprised of neritic limestone and fluvial–lacustrine clastic rocks (lower) and a flysch turbidite formation (upper). Pillow basalt and basaltic proclastics rocks up to

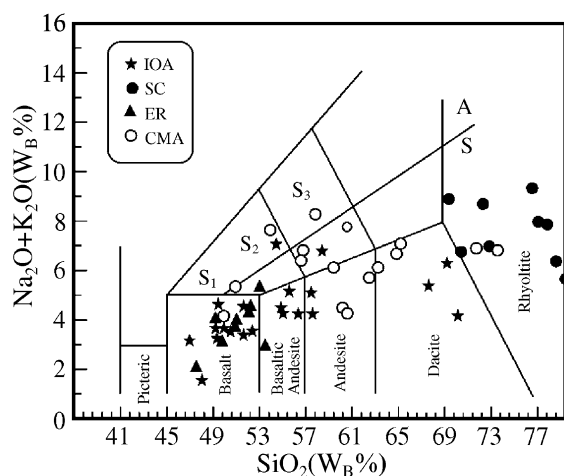


Fig. 8.  $\text{SiO}_2$  versus  $\text{Na}_2\text{O} + \text{K}_2\text{O}$  for volcanic rocks in the Jinshajiang orogenic belt (JOB) (Compositional fields after Le Bas et al., 1986). IOA—*intra-oceanic arc volcanics*; CMA—*continental margin arc volcanics*; SC—*syn-collisional volcanics*; ER—*extensional rift volcanics*.

2300-m thick occur in the center of the basin. The bimodal suite, characterized by basalt and granitic porphyry, is stratigraphically comparable with the bimodal volcanic associations of the southern segment. The sequence in the Zhaokalong–Dingqinlong basin also overlies unconformably the Proterozoic and Paleozoic strata. The sequence consists of basal molasses formation and a volcanic secession more than 300-m thick. Red-grey clastic molasses at the base of the basin is overlain by the thinly bedded, neritic limestone with minor intermediate-acidic volcanic rocks. The volcanic succession is dominated by andesitic and dacitic rocks in conjunction with clastic rocks and lenticular limestone. The pyroclastic facies and calc-alkaline andesite–dacite–rhyolite composition of this succession are comparable with the uppermost unit of the Reshuitang and Jijiading basins.

## 5. Petrology and geochemistry of volcanic rocks in the JOB

The volcanic rocks of the JOB are divided into four volcanic–tectonic groups: *intra-oceanic arc*, *continental margin arc*, *syn-collisional* and *extensional rift* volcanic rocks. This subdivision is based on spatial-

temporal distribution, rock association and geochemical features of volcanic rocks.

### 5.1. *Intra-oceanic arc volcanic rocks*

The Permian volcanic rocks of the Chubarong–Dongzhulin area (Fig. 3) represent volcanic rocks of this group. They include tholeiitic basalts and calc-alkaline basaltic andesite, amphibole andesite and andesite (Fig. 8). The calc-alkaline volcanic rocks are characterized by low  $\text{TiO}_2$  (0.92% av.), low  $\text{K}_2\text{O}$  (1.19% av.), high  $\text{Na}_2\text{O}$  (2.94% av.) and high  $\text{FeO}^*/\text{MgO}$  (1.46 av.), showing geochemical characteristics similar to those of *intra-oceanic arc volcanic rocks* (e.g., Perfit et al., 1980). The tholeiitic basalts are transitional between *island-arc basalt* and *MORB* (Fig. 9). These volcanic rocks, although affected by regional alteration, usually show light REE enriched patterns ( $\text{La}/\text{Yb}_N = 1.44\text{--}9.52$ ) (Fig. 10a). Slight to moderate depletion in MREE for these rocks (Fig. 10a) suggest the fractionation of amphibole from the magmas. Compared with *MORB*, the volcanic rocks in the area are enriched in LILE (Rb, Ba and K) and depleted in Y, Yb, Sc and Cr, and have similar abundances of HFSE (Nb, Ta, Zr, Hf and P). Strong positive anomalies for K, Rb, Ba and Th (Fig. 11a) in these volcanic rocks are characteristic of arc magmas (Nakamura, 1985) and imply that their source had

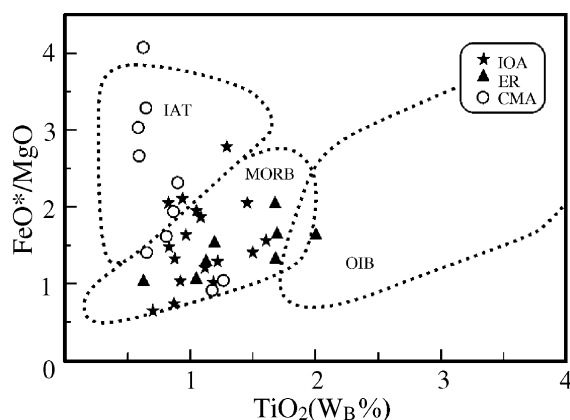


Fig. 9.  $\text{TiO}_2$  versus  $\text{FeO}^*/\text{MgO}$  for volcanic rocks in the Jinshajiang orogenic belt. IAT—*island-arc basalt*; MORB—*mid-ocean ridge basalt*; OIB—*ocean-island basalt*. IOA—*intra-oceanic arc volcanics*; CMA—*continental margin arc volcanics*; SC—*syn-collisional volcanics*; ER—*extensional rift volcanics*.

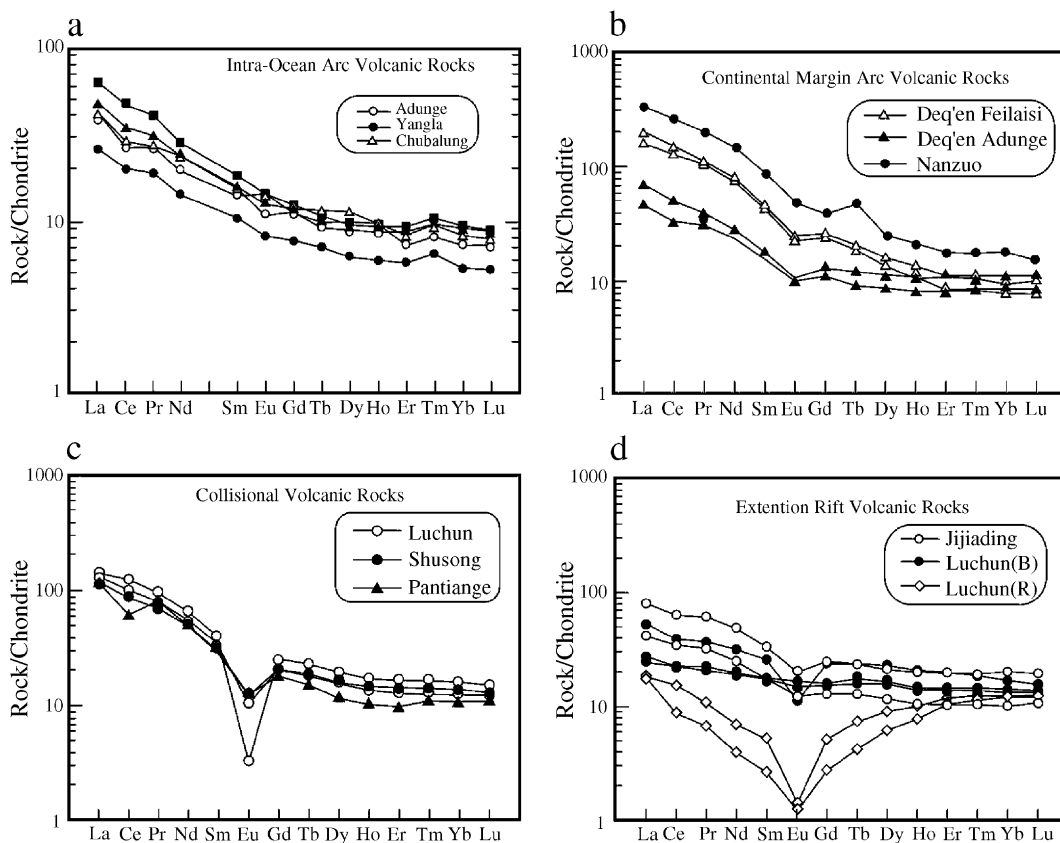


Fig. 10. REE patterns of the volcanic rocks in the Jinshajiang orogenic belt.

been metasomatized by the components ( $H_2O$ , Rb, Ba, K, LREE, etc.) derived from the subducted oceanic slab (Tatsumi, 1983, 1986).

### 5.2. Continental margin arc volcanic rocks

Volcanic rocks from the Jidonglong Formation ( $P_1$ ) and Shamu Formation ( $P_2$ ) in the Deqen–Jamda are typical of rocks of an active continental margin. The Early Permian volcanic rocks are predominately calc-alkaline, whereas the late Permian volcanic rocks are both calc-alkaline and shoshonitic (Fig. 8). The volcanic association is characterized by high  $Al_2O_3$  (11.82–15.32%), low  $TiO_2$  (0.64–1.33%) and high  $FeO^*/MgO$  ratio, similar to typical arc volcanic rocks (Fig. 9). Early Permian calc-alkaline volcanic rocks have similar total REE contents and patterns to intra-oceanic arc volcanic rocks mentioned above (Fig. 10b), whereas late Permian calc-alkaline and shosho-

nitic rocks show strong LREE-enrichment patterns and higher total REE contents (Fig. 10b), although they have similar HREE contents. Strong positive anomalies for the LILE, negative anomalies for Ti, Y, Yb, Sc and Cr and weak negative anomalies for Nb, Ta and P in the normalized abundance pattern (NAP) diagram (Fig. 11b) suggest that these volcanic rocks share arc magmatic affinity.

### 5.3. Syn-collisional volcanic rocks

The Early–Middle Triassic dacitic–rhyolitic rocks from southern Deqen and northern Jamda have 70.8–78.8 wt.%  $SiO_2$ , 2.6–5.3 wt.%  $K_2O$ , 0.68–3.38 wt.%  $Na_2O$  and 1.2–1.7  $Al/(Na+K+Ca/2)$  ratios. These characteristics are similar to collisional volcanic rocks in western United States (e.g., Ewart, 1979). Such volcanic rocks have LREE-enriched patterns with strong negative Eu anomalies ( $\delta Eu = 0.41–0.65$ )

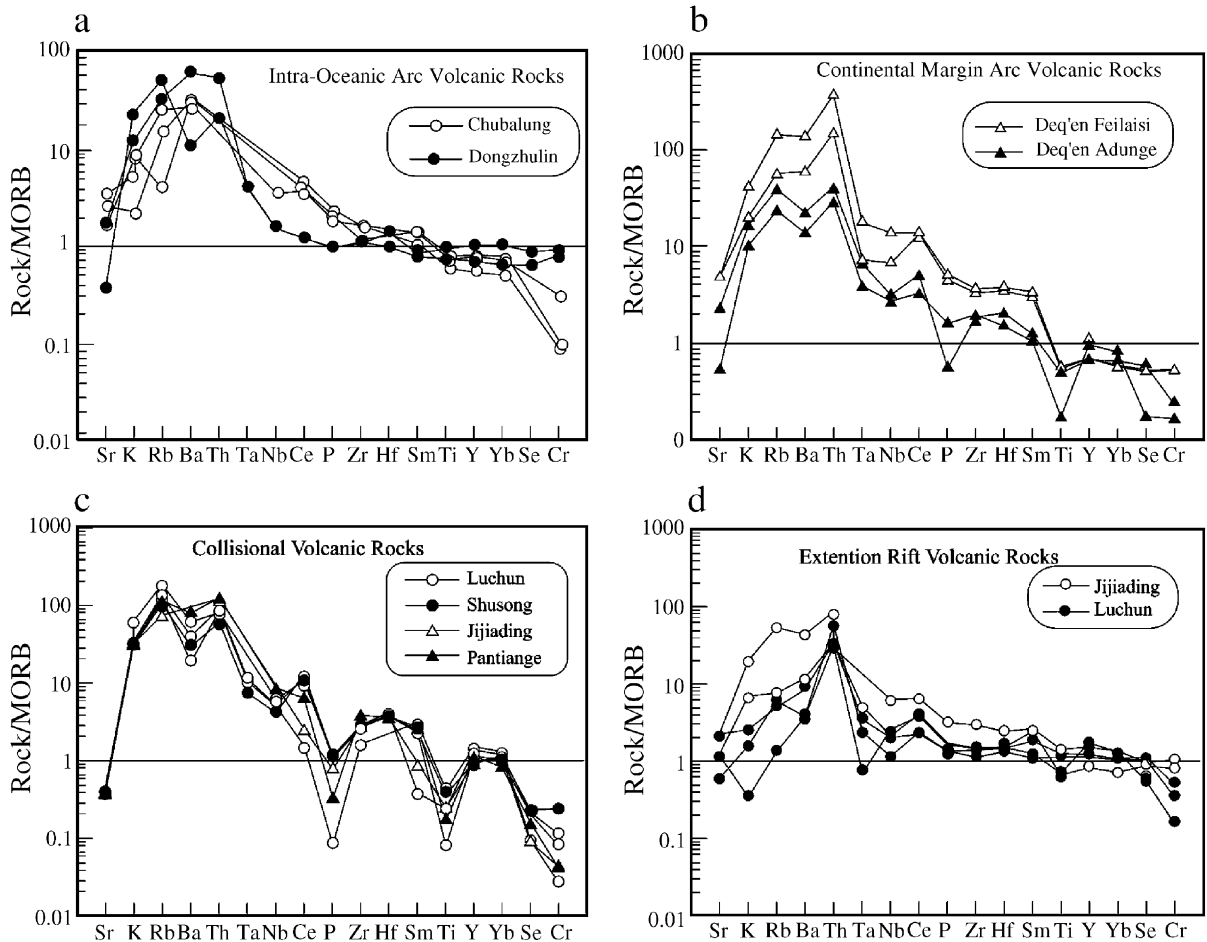


Fig. 11. Normalized abundance patterns (NAP) by N-MORB for the trace elements of volcanic rocks in the Jinshajiang orogenic belt (JOB).

(Fig. 10c). Strong negative anomalies for P, Ti, Sc and Cr and positive anomalies for LILE and HFSE (Zr, Hf) (Fig. 11c) indicate that the N-MORB normalized abundance pattern for these trace elements is very similar to that of collisional volcanic rocks (Mo et al., 1993). The volcanic rocks yield an initial  $^{87}\text{Sr}/^{86}\text{Sr}$  value of 0.7213, and give  $\epsilon_{\text{Sr}(t)}$  and  $\epsilon_{\text{Nd}(t)}$  values of 242.19 and  $-10.02$ , respectively (Wei, 1999), suggesting generation of these volcanic rocks by crustal anatexis.

#### 5.4. Extensional rift volcanic rocks

Late Triassic volcanic rocks in the Deqen area are bimodal, whereas in the Jamda area, pillow tholeiite

basalt and andesitic–dacitic–rhyolitic volcanic rocks are predominant.

The basalts in the Deqen bimodal association are tholeiitic (Fig. 8), and differ from intra-oceanic arc and continental margin arc basalts in displaying moderate  $\text{TiO}_2$  (1.44–1.69 wt.%), low  $\text{K}_2\text{O}$  (0.16–0.58 wt.%), high  $\text{Na}_2\text{O}$  (3.14–3.2 wt.%) and low  $\text{FeO}^*/\text{MgO}$  (1.49–1.67). This indicates that these basalts are geochemically similar to the MORB (Fig. 9). Although the rhyolite is also characterized by high- $\text{K}_2\text{O}$  (4.68–5.68 wt.%) and  $\text{Al}_2\text{O}_3$  (12.4–14.1 wt.%), it still differs from syn-collisional rhyolite in having relatively high  $\text{FeO}^*$  (6.3 wt.%), high  $\text{FeO}^*/\text{MgO}$  (6.76) and low  $\text{Na}_2\text{O}$  (0.5–1.9 wt.%). The tholeiite has flat REE pattern ( $\text{La}/\text{Yb}_\text{N} = 1.8\text{--}4.2$ ), which is

different from island arc basalt (Fig. 10d). The NAP diagram shows that the trace elements abundances are comparable with those of MORB except for relatively enriched LILE and Th (Fig. 11d). The initial  $^{87}\text{Sr}/^{86}\text{Sr}$  ratios for the basalt range from 0.7077 to 0.7099, whereas  $\varepsilon_{\text{Sr}}(t)$  and  $\varepsilon_{\text{Nd}}(t)$  vary in the range of 48.6–

81.2 and  $-2.56$ – $4.49$ , respectively, suggesting a magmatic source close to enrichment mantle (i.e., EM II; Wei, 1999). The relative enrichment of LILE in the basalt indicates the contribution of crustal materials to the magmatic source. The rhyolite from the bimodal suite has a swallow-like REE partition,

Table 2

Major, trace and rare-earth elements analysis of the representative volcanic rocks in the Jinshajiang orogen

	Intra-oceanic arc volcanics					Continental margin arc volcanics					Syn-collision volcanics		
	Amphibole andesite	Amphibole andesite	Meta-andesite	Meta-diabase	Diabase	Basaltic andesite	Diabase	Shoshonite	Andesite	Dacite	Dacite	Rhyolite	Rhyolitic porphyry
SiO <sub>2</sub>	54.30	57.16	57.95	42.72	64.08	55.78	56.49	54.96	56.82	60.80	71.27	77.92	67.47
TiO <sub>2</sub>	0.94	0.83	1.01	0.69	0.57	0.84	0.72	0.64	0.75	0.86	0.57	0.13	0.60
Al <sub>2</sub> O <sub>3</sub>	17.95	16.73	14.80	15.19	13.97	11.82	14.84	15.32	18.89	13.79	13.21	11.63	14.10
Fe <sub>2</sub> O <sub>3</sub>	2.12	0.87	1.87	2.03	1.05	1.31	1.12	5.37	1.97	1.72	0.60	0.50	1.04
FeO	7.11	5.27	6.96	5.23	2.98	5.77	5.87	2.43	3.85	4.17	2.72	0.93	2.50
MnO	0.15	0.11	0.15	0.16	0.06	0.12	0.15	0.07	0.07	0.09	0.05	0.01	0.03
MgO	4.32	2.97	3.92	11.48	2.79	7.13	4.38	2.22	3.49	2.48	0.83	0.39	1.47
CaO	7.24	7.26	5.34	11.04	3.96	4.97	5.17	3.18	3.84	3.37	1.36	0.65	1.73
Na <sub>2</sub> O	2.83	3.98	3.05	1.89	3.02	0.79	1.35	1.19	4.29	5.63	1.78	2.07	1.73
K <sub>2</sub> O	1.47	2.63	1.20	1.16	2.03	3.20	6.64	10.53	1.57	0.61	5.03	4.15	4.68
P <sub>2</sub> O <sub>5</sub>	0.13	0.14	0.21	0.14	0.14	0.55	0.63	0.58	0.20	0.19	0.13	0.04	0.17
H <sub>2</sub> O <sup>+</sup>	–	–	3.06	2.85	2.65	4.17	1.92	1.29	3.55	1.40	1.48	1.06	2.13
CO <sub>2</sub>			0.70	0.09	2.050	3.23	0.20	1.73	0.09	4.40	0.75	0.32	1.80
Σ	98.56	97.95	100.22	99.67	99.80	99.68	99.48	99.51	99.38	99.51	99.78	99.80	99.45
La	15.60	14.90	23.28	9.52	21.67	60.22	74.78	126.40	17.82	25.80	46.23	54.83	43.22
Ce	25.20	27.60	44.56	19.26	39.31	126.3	147.30	257.00	33.44	56.71	93.13	124.70	84.49
Pr	3.68	3.74	5.62	2.61	4.20	15.05	15.92	27.38	4.31	6.97	10.02	13.83	9.58
Nd	13.90	17.10	20.13	10.26	14.65	58.17	57.51	105.82	17.03	31.87	36.74	49.43	35.46
Sm	3.21	3.69	4.24	2.41	2.88	10.59	10.11	20.06	3.55	7.88	7.36	9.48	7.10
Eu	1.27	1.09	1.25	0.71	0.62	2.07	1.97	4.17	0.94	1.56	0.89	0.29	1.11
Gd	3.42	3.67	3.81	2.35	2.84	8.26	7.54	12.41	3.48	8.49	6.41	8.06	6.37
Tb	0.57	0.67	0.62	0.41	0.46	1.18	1.06	2.72	0.53	1.29	1.05	1.34	1.15
Dy	3.78	4.32	3.64	2.39	2.69	6.29	5.08	9.45	3.48	9.38	6.45	7.85	6.49
Ho	0.82	0.82	0.79	0.50	0.55	1.17	0.94	1.81	0.73	2.19	1.28	1.55	1.33
Er	2.06	1.80	2.31	1.43	1.51	3.02	2.28	4.26	2.16	5.53	3.70	4.37	3.74
Tm	0.34	0.29	0.37	0.23	0.25	0.44	0.34	0.60	0.34	0.84	0.58	0.69	0.60
Yb	2.06	1.80	2.33	1.32	1.50	2.38	1.91	3.70	2.26	5.62	3.58	4.19	3.58
Lu	0.30	0.28	0.34	0.20	0.24	0.39	0.31	0.63	0.34	0.70	0.53	0.60	0.54
Y	19.60	19.00	20.06	12.66	15.62	32.01	25.12	37.60		48.47	37.66	44.93	37.71
Sr			406.0	262.0	181.0	289.0	638.0	147.0	275	90.0	61.0	36.0	39.0
Rb			7.3	48.9	56.3	118.0	304.0	309.0	48	24.0	197.4	214.5	189.9
Ba			610.0	479.0	552.0	1191.0	2729.0	2511.0	290	84.0	781.0	363.0	586.0
U			–	8.0	7.3	6.5	10.5	18.0		5.0	17.2	26.5	11.5
Th			–	–	0.3	31.6	78.2	50.0	5.9	8.0	5.3	8.1	–
Nb			–	–	0.5	1.2	3.2	5.0	9.5	5.0	1.3	2.0	1.2
Ta			11.7	7.9	10.4	24.0	46.9	26.0	–	16.0	15.9	15.7	13.5
Zr			131.0	79.0	167.0	280.0	318.0	288.0	169	378.0	260.0	137.0	221.0
Hf			–	–	4.6	8.2	8.7	9.0	3.7	10.0	7.8	5.2	7.8
Sc			–	28.6	10.8	23.4	21.7	40.7	–	17.8	7.6	3.8	9.0
Cr			68.0	442.0	65.8	127.5	63.0	57.0	41.4	41.0	29.0	7.0	63.0
Location	Adenge	Yagra	Chubalung		Dongzhulin	Feilaisi		Nanzuo	Adenge	Nanzuo	Luchun		Shusong

\*Major elements were analyzed by wet-method, trace elements were analyzed by ICP-MS.

and displays a conspicuous MREE depletion and negative Eu anomaly ( $\delta\text{Eu} = 0.34$ ) (Fig. 10d). Whether this REE partition pattern is caused by intense hydrothermal alteration or fractional crystallization of MREE-bearing hornblende is unknown. However, the initial  $^{87}\text{Sr}/^{86}\text{Sr}$  ratio (0.7099),  $\epsilon_{\text{Sr}}(t)$  (80.15) and

$\epsilon_{\text{Nd}}(t)$  values ( $-9.93$ ) for these rhyolites suggest that they share a possible magmatic source with associated basalt in the area (Wei, 1999).

The pillow basalt in the Jamda area is tholeiitic, and the major and trace elements exhibit transitional characteristics between island arc tholeiite and mid-

Extension rifting volcanics												
Rhyolite	Altered rhyolite	Rhyolite	Altered rhyolite	Altered basalt	Diabase	Diabase	Basalt	Basalt	Rhyolite	Rhyolitic porphyry	Andesite	Rhyolite
78.75	70.75	74.60	69.25	49.98	51.37	50.16	48.00	45.34	76.34	67.47	66.00	74.80
0.29	0.38	0.35	0.53	1.60	1.43	1.02	1.36	1.85	0.36	0.60	0.69	0.16
11.30	13.81	12.42	12.97	14.72	14.24	16.18	15.07	16.00	12.69	14.10	12.83	11.55
0.81	2.57	0.55	5.04	2.16	0.92	1.25	3.20	3.09	0.86	1.04	1.49	1.97
0.45	0.90	1.83	1.55	10.34	10.13	6.95	7.57	9.57	0.44	2.50	2.10	1.85
0.01	0.07	0.03	0.06	0.20	0.20	0.21	0.17	0.19	0.02	0.03	0.07	0.06
0.15	0.21	0.61	0.93	7.05	6.29	7.93	7.19	7.55	0.18	1.47	5.07	0.92
0.13	0.29	1.01	0.24	5.20	10.19	8.36	8.47	4.52	0.17	1.73	0.87	0.21
0.68	3.38	1.93	0.49	2.97	1.77	1.51	2.86	2.78	1.53	1.73	1.94	4.52
5.32	5.06	4.59	5.68	0.20	0.44	2.68	0.55	0.95	4.80	4.68	3.70	3.06
0.04	0.10	0.09	0.11	0.16	0.19	0.21	0.23	0.31	0.05	0.17	0.11	0.01
1.42	1.46	1.27	2.32	4.70	2.38	3.24	4.26	6.01	1.78	2.13		
0.00	0.04	0.54	0.03	0.58	0.24	0.04	0.43	0.43	0.21	1.80		
99.35	99.02	99.79	99.16	99.83	99.79	99.74	99.36	97.93	99.42	99.45		
42.87	12.69	47.43	7.08	9.78	16.57	15.43	30.12	30.12	27.78	43.22	16.50	42.58
60.97	25.21	96.77	11.74	21.77	34.65	32.75	59.59	59.59	43.09	84.49	38.41	89.22
10.43	3.75	10.69	1.21	2.90	4.34	4.22	8.04	8.04	7.09	9.58	4.40	8.39
37.76	14.61	39.15	3.90	13.85	18.66	16.39	33.56	33.56	26.19	35.46	17.07	28.51
7.30	3.19	7.66	0.92	3.96	4.50	3.72	7.48	7.48	5.25	7.10	3.58	4.57
1.14	0.46	0.94	0.11	1.37	1.25	1.02	1.62	1.62	0.80	1.11	1.13	0.94
5.82	2.99	6.59	1.25	5.02	5.16	3.99	7.72	7.72	4.41	6.37	3.25	3.58
0.91	0.52	1.07	0.33	0.93	0.85	0.68	1.28	1.28	0.72	1.15	0.50	0.55
4.79	3.70	6.38	3.01	6.25	5.67	4.34	8.02	8.02	4.25	6.49	2.88	3.29
0.95	0.87	1.25	0.79	1.25	1.17	0.86	1.70	1.70	0.91	1.33	0.56	0.64
2.62	2.93	3.56	2.87	3.68	3.40	2.47	4.92	4.92	2.78	3.74	1.53	1.80
0.46	0.48	0.56	0.50	0.58	0.50	0.4	0.75	0.75	0.47	0.60	0.25	0.30
2.87	3.41	3.42	3.25	3.54	3.09	2.35	4.72	4.72	3.14	3.58	1.47	1.82
0.46	0.51	0.52	0.50	0.54	0.53	0.39	0.70	0.70	0.49	0.54	0.24	0.30
27.9	26.1	36.2	25.0	35.6	32.1	24.75	44.4	44.38	27.0	37.7	16.21	18.2
55.0	129.0	64.5	28.5	185.5	189.0	182.0	127.0	127.0	92.0	39.4		
200.7	15.7	283.3	237.3	6.0	9.0	109.0	14.3	14.0	178.9	189.9		
1676.0	1950.0	816.0	858.5	117.5	382.0	801.0	203.0	203.0	1813.0	586.0		
28.0	22.0	5.1	4.1	0.3	0.3	14.4	–	6.0	–	–		
–	–	20.3	15.1	10.9	11.7	0.3	6.0	–	25.0	11.5		
–	–	17.5	16.9	5.3	10.0	0.7	19.5	–	26.2	13.5		
28.2	24.1	1.4	1.7	0.5	0.9	8.1	–	19.5	–	1.2		
377.0	340.0	290.5	278.5	122.0	157.0	127.0	256.0	256.0	358.5	221.0		
8.0	7.2	8.2	7.5	3.8	4.3	3.5	5.5	5.5	7.6	7.8		
6.2	6.9	7.9	6.5	40.1	33.9	33.5	23.3	23.3	6.6	9.0		
11.0	12.0	24.8	21.0	105.6	50.0	199.0	248.0	248.0	11.5	63.0		
Pantiange	Jijiading	Luchun				Jijiading	Pantiange			Shusong	Dingqinnong	

oceanic ridge basalt (Fig. 9, Fan, 1988). The intermediate-felsic volcanic rocks in the area are mainly calc-alkaline, and their major element chemistries are similar to those of calc-alkaline volcanic rocks in the Permian Jamda–Weixi continental margin arc (Table 2). The slightly flat REE pattern or weak enrichment in LREE for the tholeiites is quite different from other volcanic rocks in the area (Fig. 10d). The similarity in the NAP of trace elements, except for mobile LILE and Th during the alteration, between the pillow basalt and MORB (Fig. 11d) suggests a strong rifting event, under which partial melting of MORB-like mantle took place to form the pillow basalts.

## 6. Discussion

### 6.1. Tectono-magmatic evolution inferred from volcanic–sedimentary sequences

The JOB is one of the important belts in the Himalayan–Tibetan Orogen. It has a complex tectonic history and evolution from a Permian arc-related to subduction of the Jinshajiang oceanic slab, Early–Middle Triassic arc–continent collision, through Late Triassic post-collisional extension to final intra-continent convergence and large-scale strike-slip movement during the Himalayan period (Tertiary).

The further spreading of initial Jinshajiang oceanic basin formed along the western margin of the Yangtze continent during the Devonian period (Liu et al., 1993; Mo et al., 1993; Wang et al., 1999b) formed a mature ocean basin during the Carboniferous–Permian periods. Evidence for this is preserved in Paleozoic ophiolite and ophiolitic mélange zone (Fig. 12; Liu et al., 1993; Mo et al., 1993; Wang et al., 1999b). In the Early Permian, westward subduction of the oceanic slab has occurred at the intra-oceanic fracture zones, and resulted in the development of the Chubarong–Dongzhulin intra-oceanic arc and the Xiquhe–Jiyidu back-arc basin. In the intra-oceanic arc, an island-arc volcanic sequence composed of tholeiitic to calc-alkaline basalt–basaltic andesite–andesite–dacite developed. In the back-arc basin, an oceanic volcanic–sedimentary sequence comprising a sheeted diabase dike swarm, tholeiite and abyssal or bathyal flysch formations occurred (Mo et al., 1993). By the end of the Early Permian, the oceanic plate was

subducted extensively towards the Changdu continental block, resulting in the formation of a continental margin arc, i.e., the Permian Jamda–Deqen–Weixi Arc (Mo et al., 1993; Liu et al., 1993).

During the Triassic, significant changes occurred in the trench–arc–basin system. The arc–continent collision at the end of the late Permian caused the closure of the Jinshajiang ocean basin, accounting for the absence of Early–Middle Triassic strata in the area. The Early–Middle Triassic syn-collisional felsic and andesitic volcanic rocks are developed around the Shusong–Tongyou area (southern segment) and the Jamda–Qizhong area (northern segment), respectively.

In the Late Triassic, crustal extension commenced in the orogenic belt, possibly due to mountain-root delamination (Kay, 1994; Kay and Kay, 1994; Dong, 1999) or breaking-off of the subducting slab (Sacks and Secor, 1990; Davies and Blanckenburg, 1995) underneath the orogenic belt. Both processes would have caused upwelling of the asthenosphere, resulting in the lithosphere thinning and heating of the lower crust, thus facilitating rapid crustal uplift and extension. The combination of depression and heating of the lithosphere caused by delamination usually results in extensive underplating of basaltic magma and eruption of shoshonitic magma (Kay, 1994; Kay and Kay, 1994). Tomographic data for global seismicity (Fukao et al., 1994) reveal that the Tethyan subducting slabs are mostly broken and subsided back into the mantle where it is presently about 1200-km deep. The tomographic data of seismicity across the East Tibet obtained by Zhong et al. (2001) suggest that the subducting slab was broken and descended deep into the mantle. Either the lithospheric delamination or the breaking up of the subducting slab triggered extensive upwelling of asthenosphere, resulting in thinning and extension of the crust and subsequently large-scale magmatism to form extensional rift basins in the JOB since the Late Triassic (Wang et al., 1999a).

Four post-collisional extensional rift basins have been recognized along the JOB, namely the Luchun–Hongpo, the Reshuitang–Cuiyibi, the Xialaxiu–Sinda and the Zhaokalong–Jamda basins. The former two basins in the southern segment of the JOB are characterized by bimodal basalt–rhyolite and bathyal turbidite and arenaceous–pelitic flysch. Both basins

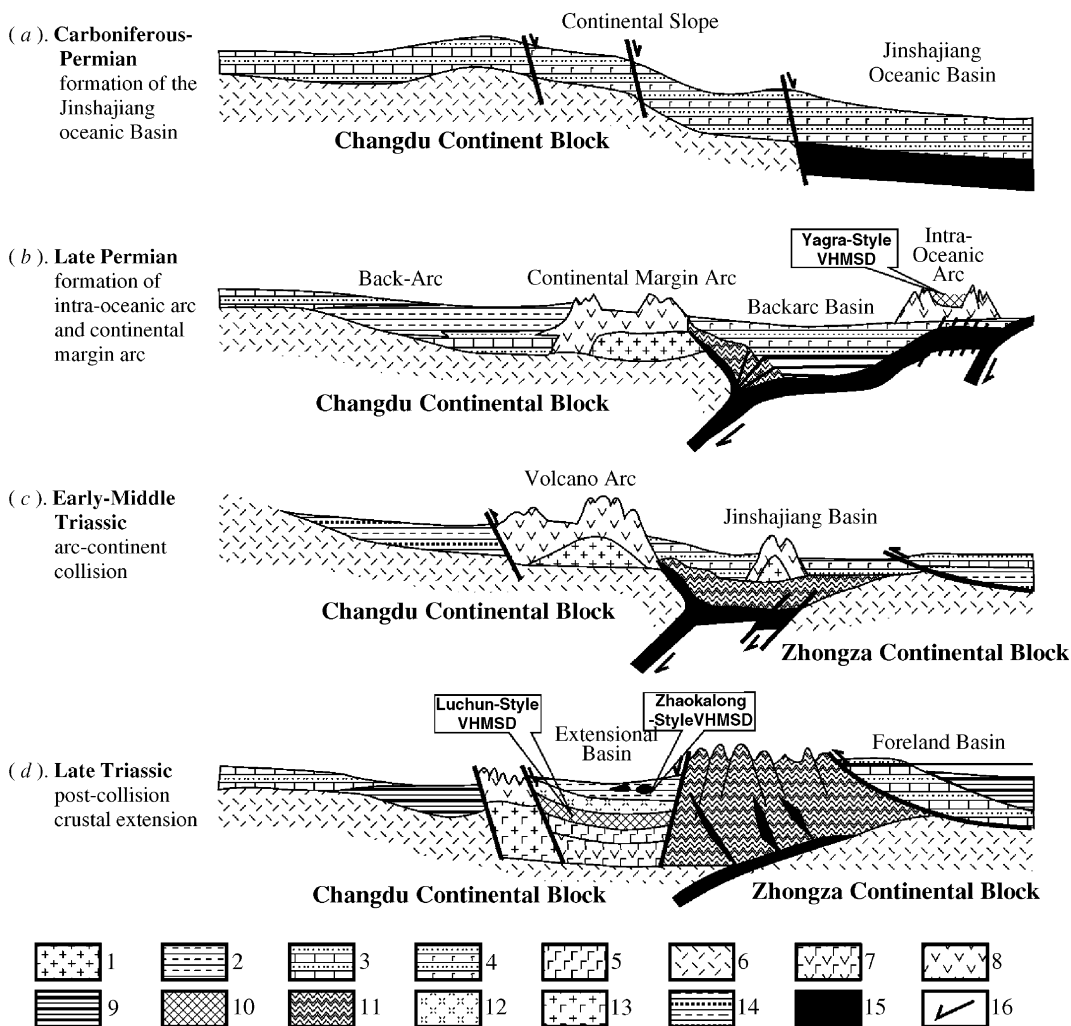


Fig. 12. Schematic tectonic evolution of the Jinshajiang orogenic belt (modified from Wang et al., 1999a). 1. Felsic intrusive rocks; 2. Continental margin clastic rocks; 3. Platform carbonate rocks; 4. Basin volcanic rocks; 5. Basalt; 6. Crustal basement; 7. Intermediate-basic arc volcanic rocks; 8. Intermediate-felsic arc volcanic rocks; 9. Abyssal flysch; 10. Orebody or deposit; 11. Structural melange; 12. Rhyolite; 13. Bimodal volcanic rocks; 14. Platform clastic rocks; 15. Oceanic crust; 16. Subduction direction.

were reduced at the end of the Triassic and infilled by shallow-marine molasses formations, with a large quantity of gypsum–barite-bearing sediments. The latter two basins occur in the northern segment of the JOB. The Xialaxiu–Sinda is a deep-water basin formed by intensive extension along the western side of the Jamda arc during the Late Triassic, producing abyssal pillow basaltic lavas, gabbro and diabase dikes. The Zhaokalong–Jamda is a shallow-marine basin resulted from the extension along the Jamda

volcanic arc during the Late Triassic, and contains a suite of shallow-marine calc-alkaline andesitic–dacitic–rhyolitic volcanic rocks and basal molasses formation.

## 6.2. Metallogenic environments and ore-horizons

VHMS deposits of the JOB occurred mainly in the late Permian marine volcanic district and Late Triassic volcanic district. These deposits were formed in intra-

oceanic arc and extensional rift environments, and occurred mainly in three host-rock units, i.e. the Permian intra-oceanic volcanic rocks, Late Triassic bimodal volcanic rocks and Late Triassic intermediate-felsic volcanic rocks (Fig. 2).

The Yagra-style VHMS deposits occur in an intra-oceanic arc environment and are hosted by late Permian arc volcanic–sedimentary sequences, consisting of arc basaltic–andesitic volcanics, black siliceous shale and metaquartzose sandstone. The shale-sandstone formation in the upper sequence, developed in a bathyal environment in the forearc region, usually is a favored horizon for VHMS deposits (Li et al., 2000). Therefore, mineralization probably occurred in a deep-water forearc environment on the eastern flank of the volcanic arc. Active hydrothermal system and base-metal deposits have been discovered in similar environments on the modern sea floor (Izasa et al., 1999). A typical example is a submarine caldera in the Izu–Bonin forearc that contains a giant Kuroko-type deposit with ore reserves equivalent to 80% of the total ore reserves of the known 432 Kuroko deposits in the world (Izasa et al., 1999).

In the rift basin environment where post-collisional extension was active, two distinctive types of VHMS deposits have been recognized: deep-marine deposits and shallow-water deposits. The former is represented by the Luchun copper deposit in the Luchun–Hongpo basin in the south, the latter is represented by the Zhaokalong deposit in the Jamda–Dingqinlong basin in the north.

In the Luchun district, the host rock sequence comprises four volcanic–sedimentary units, which reflects a progression from shallow-water to deep-water and back to a shallow-water environments, and records an evolution from initial extension, through strong rifting to basin shrinking. The first unit comprises shallow-water terrigenous clastic rocks and basaltic volcanic rocks. The terrigenous clastic rocks mainly are feldspar bearing sandstone, feldspar–quartz graywacke and silty shale with cross bedding, suggesting a shallow-water environment during the initial extension. The second unit comprises arenaceous–pelitic flysch, tuffaceous turbidite, and tholeiite and tuffaceous rocks with graded bedding and ripple bedding deposited in a deep-water environment. The third unit hosts for VHMS deposits, and comprises bimodal volcanic suite, bathyal tuffaceous

turbidite and arenaceous and pelitic flysch formations. The volcanic–sedimentary sequence suggests a deep-water rifting basin environment, under which the Luchun-style VHMS deposits formed. The bimodal suite consists of tholeiitic volcanic rocks with associated gabbro and diabase dikes and lesser rhyolitic volcanic rocks hosting VHMS deposits. The fourth unit is mainly composed of shallow-water clastic rocks and a rhyolitic volcanic complex, which are overlain by the Late Triassic neritic molasses clastic rocks and gypsum-bearing sediments. The siderite lenses have an exhalative origin in a shallow-water oxidizing environment. They are closely associated with the rhyolitic volcanic rocks, and constitute a favored ore-horizon for the Chugezha-style VHMS deposits.

In the Jamda–Dingqinlong basin, the favorable ore horizon for the VHMS deposits roughly coincides with that for the Chugezha-style deposits. The VHMS deposits occur in the northern part of the basin, and are hosted in volcanic–sedimentary sequence of the Upper Triassic. In the Zhaokalong district, ore-bearing sequence consists of thickly bedded crystalline limestone and massive dolomite, purple dacitic–rhyolitic pyroclastic volcanic rocks, thinly bedded grey sandstone and shale. The host rocks are mainly sandstone, siltstone, shale and siderite-rich bed. Metallic sulfides occur primarily as veined, stockwork and densely disseminated, strictly occurring within the siderite-rich beds. In the Dingqinlong district, the host rocks are grey dacitic–rhyolitic pyroclastic volcanic rocks and strongly altered siliceous beds and thickly bedded marble and dolomite overlain by rhyolitic volcanic tuff. The orebodies are stratified and are folded as their host rocks.

Compared with the Luchun deposit, the Zhaokalong and Dingqinlong deposits occur in a relatively shallow-water volcanic environment. There are several lines of evidence to support the view: (1) The host volcanic rocks are mainly pyroclastics with ignimbritic texture and purplish grey–dark red layers at the upper part (Wang et al., 2000), and conformably overlie the red–purplish subaerial and/or molasses formations in the Upper Triassic; (2) Siderite-rich beds are a major host rock for massive sulfide orebodies, and are important ore-equivalent horizons closely associated with massive sulfide deposits, suggesting a strongly oxidizing environment during

hydrothermal activity and mineralization. Massive dolomite usually occurs at the top or on the edges of massive sulfide bodies in the Zhaokalong and Dingqinlong deposits, as is common in many shallow-water VHMS deposits (De Carvalho, 1991; Galley et al., 1993; Halley and Roberts, 1997); (3) The strong silicification of the footwall host rocks is typical of shallow-water VHMS deposits (Halley and Roberts, 1997). In a shallow-water environment, boiling will take place in a sea-floor hydrothermal system with 300–350 °C (Lydon, 1988). As a result, large amounts of SiO<sub>2</sub> and base-metal sulfides will be deposited on the sea floor to produce highly silicified rocks and stringer-stockwork and disseminated sulfide bodies (Lydon, 1988; Large, 1992). In the Zhaokalong district, stringer-stockwork and disseminated base-metal sulfides are concentrated within siderite-rich beds, whereas in the Dingqinlong district, base-metal sulfide bodies occur in highly silicified rocks.

### 6.3. Post-collisional crustal extension setting—a new environment for VHMS deposits

The post-collisional crustal extension, as a significant tectonic event in orogens, provides a favorable environment for the VHMS deposits (Crawford and Berry, 1992; Crawford et al., 1992, 2000). For example, the intense post-collisional crustal extension in the Middle–Late Cambrian resulted in the formation of Mount Read Volcanics on the passive continental margin and associated Cambrian VHMS metallogenic belts in western Tasmania, Australia (Crawford and Berry, 1992; Crawford et al., 1992).

A similar tectono-magmatic event also took place in the JOB, southwestern China. Westward subduction of the Jinshajiang oceanic crust at the end of Early Permian resulted not only in the formation of the Chubarong–Dongzhulin intra-oceanic arc, but also in the development of a continental margin arc on the margin of the Changdu block. The arc–continent collision in the Early–Middle Triassic led to the closing of the Jinshajiang oceanic basin and to the westward obduction and emplacement of an ophiolite mélangé. This was also associated with eruption of high-K felsic volcanic rocks, formation of the foreland basin and overall uplift of the active continental margin. In the Late Triassic, the lithospheric extension caused strong bimodal volcanism and crustal rifting to

form volcanic rift basins in the active marginal arc accompanied by strong submarine hydrothermal mineralization. As a product of post-collisional extension, Late Triassic extensional basin and ore-bearing volcanic sequences occur on a Permian active continental margin arc in the Jinshajiang orogenic belt, rather than a passive continental margin as was the case in the Mount Read Volcanics (Crawford and Berry, 1992; Crawford et al., 1992, 2000). Accordingly, we prefer to the former as the active margin type, whereas the latter is the passive margin type.

NS-trending rift basins with various depths and sizes were developed on these continental margin arcs, due to post-collisional extension at the end of the Triassic. In the early stages of the rifting of the basin, bimodal volcanism accompanied by deposition of bathyal flysch and turbidites in conjunction with sea-floor hydrothermal system occurred, and the Luchun-style VHMS deposits was formed in association with high-K rhyolitic rocks of the bimodal suite. The Cu–Zn–Pb VHMS deposits displaying characteristics of Kuroko-type deposits were formed in a deep-water volcanic environment. In the late closing stages of the basin development, high-K intermediate-felsic volcanism, accompanied by the accumulation of neritic or littoral molasses sediments and carbonate, occurred in the basin. Hydrothermal activity and metallogenic processes took place during the quiet periods of volcanism. Massive sulfide deposits were formed in the contact zones between the volcanic and overlying carbonate rocks. Metallic sulfides are exclusively hosted in stratified siderite-rich beds and/or strongly silicified rocks, showing stratabound features. Thus, these Ag-rich, Pb–Zn siderite-rich deposits were probably formed in a shallow-water environment.

## 7. Conclusions

The JOB of southwestern China is located along the eastern margin of the Himalayan–Tibetan Orogen, and includes a collage comprised of the Changdu continental block joined by Paleozoic Jinshajiang ophiolitic sutures and Permian Jamda–Weixi volcanic arc. Three major tectonic stages have been recognized based on the volcanic–sedimentary sequence and the geochemistry of volcanic rocks in the belt, i.e.,

Permian volcanic arc, Early–Middle Triassic syn-collision and late Triassic post-collisional extension. Westward subduction of the Paleozoic Jinshajiang oceanic plate at the end of Permian resulted in the formation of the Chubarong–Dongzhulin intra-oceanic arc and Jamda–Weixi volcanic arc on the eastern margin of the Changdu continental block. Collision between the volcanic arc and Yangtze continent during Early–Middle Triassic periods caused the closing of the Jinshajiang oceanic basin and the eruption of high-Si and -Al potassic rhyolitic rocks locally along the Permian volcanic arc. Probably due to the slab breakoff or mountain-root delamination under the orogenic belt, post-collisional crustal extension occurred at the end of Triassic, and formed a series of rift basins on the continental margin arc.

A significant potential for VHMS metallogenic belt occurs in the submarine volcanic districts of the JOB. The Paleozoic Yagra-style VHMS deposits occur in the Permian intra-oceanic arc and are hosted by calc-alkaline andesitic volcanic rocks, overlying black shale. Almost all Mesozoic VHMS deposits occur in the post-collisional extension environment and cluster in the Late Triassic rift basins with various water-depth and sizes. The Luchun-style deposits are related to marine bimodal volcanism in the Late Triassic, and occur in the rhyolitic volcanic pile and are closely associated with chert lens and banded dolomite. These deposits display characteristics of Kuroko-type deposits, and form in relatively deep-water volcanic environment. The Chugezha-style deposits occur at upper volcanic succession within the rifting basins, and are hosted by dacitic–rhyolitic pyroclastics with ignimbritic texture and sandstone-shale formation. Massive sulfide orebodies of these deposits occur in the siderite-rich lenses associated with strongly silicified pyroclastics and were formed in a shallow-water volcanic environment.

### Acknowledgements

The authors would like to thank the staff members of the Institute of Mineral Deposits, Chinese Academy of Geological Sciences (CAGS), Beijing, for constructive discussions and comments. Special thanks are due to Jocelyn McPhie, Richard Squire and Tony Crawford for their useful comments to improve the

manuscript. The manuscript benefited from the review by Ore Geology Review reviewers, Drs. Victor Maksiav and Scott Halley.

### References

- Cathles, L.M., Guber, A.L., Lenagh, T.C., Dudas, F.O., 1983. Kuroko-type massive sulfide deposits of Japan: products of an aborted island-arc rift. *Econ. Geol. Monogr.* 5, 96–114.
- Crawford, A.J., Berry, R.F., 1992. Tectonic implications of Late Proterozoic–Early Palaeozoic igneous rock associations in western Tasmania. *Tectonophysics* 214, 37–56.
- Crawford, A.J., Corbett, K.D., Everard, J., 1992. Geochemistry and tectonic setting of a Cambrian VHMS-rich volcanic belt: the Mount Read Volcanics, western Tasmania. *Econ. Geol.* 87, 597–619.
- Crawford, A.J., Gifkins, C.C., Allen, R.L., 2000. Tectonic setting of mineralization, Mt. Read Volcanics, western Tasmania. In: Gemmell, J.B., Pongratz, J. (Eds.), *Volcanic Environments and Massive Sulfide Deposits*, International Conference, 16–19 November, 2000, Centre for Ore Deposit Research, University of Tasmania, Hobart, Tasmania, Australia, pp. 93–95.
- Davies, J.H., Blanckenburg, F.V., 1995. Slab breakoff: a model of lithosphere detachment and its test in the magmatism and deformation of collision orogens. *Earth Planet. Sci. Lett.* 129, 85–102.
- De Carvalho, D., 1991. A case history of the Neves-Corvo massive sulfide deposit, Portugal, and implications for future discoveries. *Econ. Geol. Monogr.* 8, 314–334.
- Dong, S.-W., 1999. Tectono-magmatic evolution and metallogeny in the orogens. In: Chen (Ed.), *Theories and Technology of Mineral Resource Exploration and Assessment*. Earthquake Press, Beijing, pp. 74–82 (in Chinese).
- Ewart, A., 1979. A review of the mineralogy and chemistry of Tertiary-recent dacitic, rhyolitic and related salic volcanic rocks. In: Barker, F. (Ed.), *Trondhiemites, Dacites and Related Rocks*. Elsevier, New York, pp. 13–21.
- Fan, L., 1988. Petrology and geodynamic setting of basalts in Chesuo, East Tibet. Unpub. MS thesis, China University of Geosciences (in Chinese with English abstract).
- Fouquet, Y., Stackelberg, U., Charlou, J.L., Erziner, J., Herzig, P., Muhe, R., Wiedicke, M., 1993. Metallogenesis in back-arc environments: the Lau basin example. *Econ. Geol.* 88, 2154–2181.
- Franklin, J.M., Lydon, J.W., Sangster, D.F., 1981. Volcanic-associated massive sulfide deposits. *Econ. Geol.*, 485–627 (75th Anniversary Volume).
- Fukao, Y., Muruyama, S., Inoue, H., 1994. Geologic implication of the whole mantle wave tomography. *J. Geol. Soc. Jpn.* 100, 4–23.
- Galley, A.G., Bailes, A.H., Kitzler, G., 1993. Geological setting and hydrothermal evolution of the Chisel Lake and North Chisel Zn-Pb-Cu-Ag-Au massive sulfide deposits, Snow Lake, Manitoba. *Explor. Min. Geol.* 2, 271–295.
- Halbach, P., Nakamura, K., Wahsner, M., Lange, J., Sakai, H., Kaselitz, L., Hanse, R.D., Yamano, M., Post, J., Seifert, R., Michaelis, W., Teichmann, F., Kinoshita, R., Marten, A., Ishi-

- bashi, J., Czerwinski, S., Blum, N., 1989. Probable modern analogue of Kuroko type massive sulfide deposits in the Okinawa trough backarc basin. *Nature* 338, 496–499.
- Halley, S.W., Roberts, R.H., 1997. Henty: a shallow-water gold-rich volcanogenic massive sulfide deposit in Western Tasmania. *Econ. Geol.* 92, 438–447.
- Hou, Z.-Q., Mo, X.-X., Zhu, Q.-W., Shen, S.-W., 1996a. Mantle plume in the Sanjiang Paleo-Tethyan region, China: evidence from oceanic-island basalts. *Acta Geosci. Sin.* 17, 343–361 (in Chinese with English abstract).
- Hou, Z.-Q., Mo, X.-X., Zhu, Q.-W., Shen, S.-W., 1996b. Mantle plume in the Sanjiang Paleo-Tethyan region, China: evidence from mid-ocean ridge basalts. *Acta Geosci. Sin.* 17, 362–375 (in Chinese with English abstract).
- Izasa, K., Fiske, R.S., Ishizaka, O., 1999. A Kuroko-type polymetallic sulfide deposit in a submarine caldera. *Science* 283, 975–977.
- Kay, S.M., 1994. Young mafic back arc volcanic rocks as indicators of continental lithospheric delamination beneath the Argentine Puna Plateau, Central Andes. *J. Geophys. Res.* 99, 24323–24339.
- Kay, R.W., Kay, S.M., 1994. Delamination and delamination magmatism. *Tectonophysics* 219, 177–189.
- Large, R.R., 1992. Australian volcanic-hosted massive sulfide deposits: features, styles and genetic models. *Econ. Geol.* 87, 469–470.
- Le Bas, M.J., Le Maitre, R.W., Streckeisen, A., Zanettin, B., 1986. A chemical classification of volcanic rocks based on the total alkali-silica diagram. *J. Petrol.* 27, 745–750.
- Li, D.-M., Chen, K.-X., Wang, L.-Q., Xu, T.-R., Diao Z.-Z., 2000. Tectonic evolution and Cu–Au metallogeny in the Jinshajiang orogenic belt. Open file report, Chengdu Institute of Geology and Mineral Resources (in Chinese).
- Liu, Z.-Q., Li, X.-Z., Ye, Q.-T., Luo, J.-N., Shen, G.-F., 1993. Division of Tectono-Magmatic Zones and the Distribution of Deposits in the Sanjiang Area. Geological Publishing House, Beijing (in Chinese with English abstract).
- Lydon, J.W., 1988. Ore deposit models #14 volcanogenic massive sulfide deposits: Part 2. Genetic models. *Geosci. Can.* 15, 43–65.
- Mo, X.-X., Lu, F.-X., Shen, S.-Y., Zhu, Q.-W., Hou, Z.-Q., 1993. Volcanism and Metallogeny in the Sanjiang Tethys. Geological Publishing House, Beijing (in Chinese with English abstract).
- Nakamura, E., 1985. The influence of subduction processes on the geochemistry of Japanese alkaline basalts. *Nature* 316, 55–58.
- Perfit, M.R.D., Gust, A., Bence, R.J., 1980. Chemical characteristics of island-arc basalts: implications for mantle sources. *Chem. Geol.* 30, 256–277.
- Rona, P.A., 1984. Hydrothermal mineralization at seafloor spreading centers. *Earth Sci. Rev.* 20, 1–104.
- Rona, P.A., Scott, S.D., 1993. A special issue on seafloor hydrothermal mineralization: new perspectives—preface. *Econ. Geol.* 88, 1933–1976.
- Sacks, P.E., Secor Jr., D.T. 1990. Delamination in collisional orogens. *Geology* 18, 999–1002.
- Sengor, A.M.C., Natalin, B.C., 1996. Paleotectonics of Asia: fragments of a synthesis. In: Yin, A., Harrison, T.M. (Eds.), *The Tectonics of Asia*. Cambridge Univ. Press, New York, pp. 486–640.
- Tatsumi, Y., 1983. Generation of arc basalt magma and thermal structure of the mantle wedge in subduction zones. *J. Geophys. Res.* 88 (B7), 5815–5825.
- Tatsumi, Y., 1986. Chemical characteristics of fluid phase released from a subduction lithosphere and origin of arc magma: evidence from high pressure experiments and natural rocks. *J. Volcanol. Geotherm. Res.* 29, 293–309.
- Urabe, T., Marumo, K., 1992. A new model for Kuroko-type deposits of Japan. *Episodes* 14, 246–251.
- Wang, L.-Q., Pan, G.-T., Li, D.-M., 1999a. Spatial-temporal architecture and tectonic evolution of the Jinshajiang arc-basin system. *Acta Geol. Sin.* 73 (3), 206–218 (in Chinese with English abstract).
- Wang, X.-F., Metcalf, I., Jian, P., 1999b. Division of tectono-strata and geological date for the Jinshajiang suture zone. *Sci. China* 29, 290–296 (in Chinese).
- Wang, M.-J., Peng, Y.-M., Wang, G.-M., Shentu, B.-Y., Yao, P., Chen, M., 2000. Evolution and ore-forming conditions of the Changdu basin. Open file report, Chengdu Institute of Geology and Mineral Resources (in Chinese).
- Wei, Q.-R., 1999. Isotopic tracing of the volcanics and division of element geochemistry in the middle segment of the Sanjiang region. Unpublished PhD dissertation, China University of Geosciences (in Chinese with English abstract).
- Wei, J.-Q., Chen, K.-X., He, L.-Q., 1999. Tectono-magmatic type of the volcanics in the Yargla district. *Acta Geosci. Sin.* 20, 246–252 (in Chinese with English abstract).
- Ye, Q.-T., Shi, G.-H., Yie, J.-H., Yang, C.-Q., 1992. Geological Characteristics and Mineralogenic Series of the Lead–Zinc Deposits in Sanjiang Region. Scientific and Technical Publishing House of Beijing, pp. 50–75 (in Chinese with English abstract).
- Yin, A., Harrison, T.M., 2000. Geologic evolution of the Himalayan–Tibetan orogen. *Annu. Rev. Earth Planet. Sci.* 28, 211–280.
- Zhan, M.-G., Lu, Y.-F., Chen, S.-F., 1998. The Yargla Copper Deposit in Deqen, Western Yunnan. Publishing House of the China University of Geosciences, Wuhan (in Chinese with English abstract).
- Zhong, D.-L., Ding, L., Liu, F.-T., Liu, J.-H., Zhang, J.-J., Ji, J.-Q., Chen, H., 2001. Poly-layered architecture of lithosphere in orogen and its constraint on Cenozoic magmatism—example from Sanjiang and surrounding area. *Sci. China* 30, 1–8 (in Chinese).